Perveance and Beamlet Expansion Modeling of the NEXT Ion Engine

IEPC-2005-155

Presented at the 29th International Electric Propulsion Conference, Princeton University October 31 – November 4, 2005

Jerold W. Emhoff*
Johns Hopkins University Applied Physics Laboratory, Laurel, Maryland, 20723
Iain D. Boyd†
University of Michigan, Ann Arbor, Michigan, 48109
Cody C. Farnell‡and John D. Williams§
Colorado State University, Fort Collins, Colorado, 80523

The axisymmetric ion optics model *erode* is applied to the NEXT ion engine. This model is compared and contrasted to four other models in a perveance study. Although each model is different from the others, they generally produce similar results. Direct impingement of the beamlet on the accelerator grid is examined as a function of beamlet current, distance between the accelerator grid and screen grid, and the discharge potential. The *erode* model is also modified to allow expansion of the beamlet in the downstream region. This produces a potential hill in the plume region downstream of the ion optics, which more closely matches the true potential field behavior.

I. Introduction

NASA's Evolutionary Xenon Thruster (NEXT) has completed a 2000 hour wear test[1] and is currently undergoing a long-duration wear test in order to process 450 kg of xenon propellant.[2] The thruster is 40 cm in diameter, with a 3.52 A, 1800 V maximum operating condition. Computer simulations have been used to model NEXT in its entire design and testing phase to date.[3–5] However, these models have not typically been compared directly to one another in many situations. All models have been used to predict the life of the NEXT thruster, but the large variance in many parameters for the simulations causes difficulty in directly comparing the models to one another.

In this paper, several models from three different sources are compared to each other for the same geometry and input parameters. The comparison is performed via a study of the perveance behavior of a NEXT ion optics aperture. This study sheds light on how similar and different the models are in their operation.

As a second study, the expansion of a beamlet in the NEXT ion engine is simulated. In a typical simulation, the area of the domain does not increase downstream of the ion optics, and particles are not removed in any way. This results in the simulation maintaining a constant density of particles in a constant area, even though in reality the thruster has a finite beam divergence. This divergence increases the beam area and decreases the particle densities in the plume, resulting in a decrease in potential field.

The paper will begin by introducing the primary model used, *erode* . The model operation will be briefly discussed, followed by discussion of the perveance fraction and its meaning, and the operation of each model. Results will then be given for the perveance study. This will be followed by a discussion and results for simulated beamlet expansion.

*Post-Doctoral Researcher, Research and Technology Development Center, Jerold.Emhoff@jhuapl.edu
†Professor, Aerospace Engineering, iainboyd@engin.umich.edu
‡Graduate Student Research Assistant, Mechanical Engineering, ccf@engr.colostate.edu
§Assistant Professor, Mechanical Engineering, johnw@engr.colostate.edu

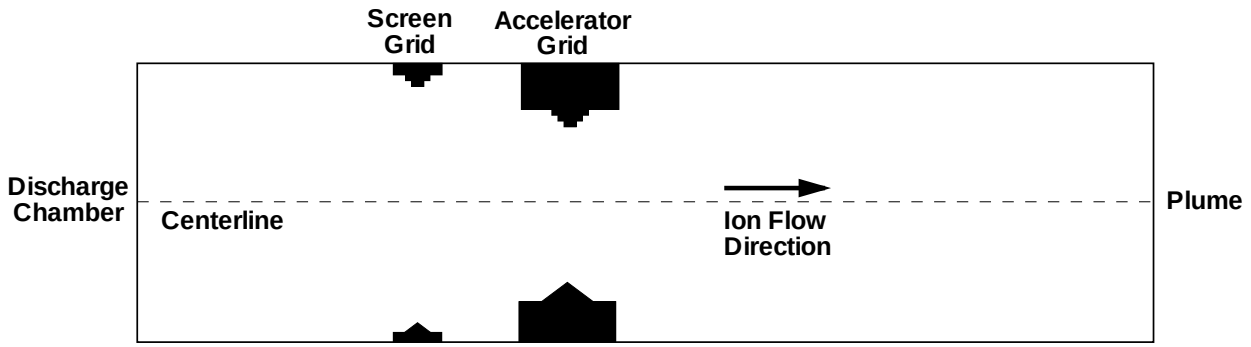

Figure 1. Schematic of the simulation domain. The upper half is the meshed simulation domain, while the bottom half is the actual domain geometry.

II. Model Operation

The computational model *erode* simulates a single 2-D axisymmetric aperture in an ion thruster. Particles are tracked via a computational mesh composed of evenly spaced rectangular cells. This mesh is also used to solve for the potential field in the domain self-consistently. The ion optics are modeled as boundary cells in the mesh, and are arranged in a stair-step pattern for the simulation of cusp structures. Figure 1 shows a typical domain, with the top half of the plot showing the meshed representation, and the bottom half showing the actual geometry. The radius of the domain is set to half the center-to-center spacing between adjacent apertures in the ion optics.

The Particle-In-Cell[6] (PIC) method is used to simulate xenon ions, xenon neutrals, and doubly charged xenon ions, although some simulations may include only xenon ions. Electrons are modeled as a fluid via the Boltzmann relation, with two reference states: one for the domain upstream of the ion optics, and one for the domain downstream of the ion optics. Particle collisions are computed via the direct simulation Monte Carlo (DSMC) method.[7] Both charge-exchange (CEX) and momentum-exchange collision types are simulated.

For simulations that do not require that the CEX current collected on the accelerator grid be modeled, neutral particles are not injected into the domain. Also, when ions neutralize on the ion optics, the particle is deleted rather than re-emitted into the domain as a neutral. This allows for a much shorter simulation as there are many fewer particles in the domain, and the ion flow reaches a steady state in only several thousand iterations, rather than tens of thousands of iterations.

The maximum power operating conditions for the NEXT thruster are typically simulated, and the centerline aperture of the thruster is normally modeled for those conditions. This involves a discharge potential of 1800 V, a screen grid potential of 1776 V, and an accelerator grid potential of -210 V. The plume plasma potential is set to about 16 V. The beamlet current for the centerline aperture is approximately 0.168 mA.

III. Perveance Modeling

One of the most basic parameters of ion optics performance is the perveance fraction. This fraction indicates the relative amount of current flowing through an aperture. For a fraction of one, the current is at the Child's Law limited current for that aperture and electric field. In the case of ion optics, very high perveance fractions result in direct impingement of beamlet ions on the accelerator grid wall, due to expansion of the beamlet. For very low perveance fractions, the beamlet will also impinge, due to over-focusing of the ions. Since any direct impingement results in large amounts of accelerator grid erosion, it is highly undesirable, and any ion thruster configuration must maintain mid-range perveance fractions in all apertures.

The perveance fraction[8] is defined as

$$f_p = \frac{j_b l_e^2}{V_T^{3/2} P_{max}}, \tag{1}$$

where

$$l_e = \sqrt{(l_g + t_s)^2 + \frac{d_s^2}{4}} \tag{2}$$

and

$$P_{max} = \frac{4\varepsilon_0}{9}\sqrt{\frac{2e}{m_i}}. \tag{3}$$

j_b is the current density upstream of the ion optics, V_T is the total voltage drop between the discharge chamber and the accelerator grid, m_i is the ion mass, l_g is the grid gap size, t_s is the screen grid thickness, d_s is the screen grid aperture diameter, and P_{max} is the theoretical maximum perveance. For xenon, P_{max} is $4.77 \cdot 10^{-9} A/V^{3/2}$.

If the current density j_b is large enough that the perveance fraction is one, then the theoretical maximum amount of current will be drawn through the ion optics. Any further increase in j_b will result in ions directly impinging on the accelerator grid, because the space charge of the ions in the aperture is too strong for the ions to be focused properly.

A. Ion Optics Models

Five different models are compared here. The *igx*[9] and *ffx*[5] models have been developed at Colorado State University. The *igx* simulation is a 3-dimensional model that makes use of symmetry to simulate a full aperture. *ffx* is fully three-dimensional without the use of symmetry, and may be used to simulate phenomena such as aperture misalignment. *igx* makes use of a cold-sheath approximation that limits the potential to at or below a reference electron potential. *ffx* uses the Boltzmann relation to model electrons as a fluid, the same as *erode*, with the exception that the exponential is linearized when the potential is higher than the reference plasma potential. Both *igx* and *ffx* inject ions at the upstream edge of the domain and allow a sheath to form self-consistently. Both models are also capable of simulation of charge-exchange ions by modeling the neutral density as a fluid and calculating collision frequencies based on the ion and neutral densities. *ffx* can also simulate cusp structures on the ion optics using a stair-step pattern, similar to *erode*. These models are different from the others in that the target beamlet current is set at the beginning of a simulation and the upstream ion density is determined by the final flow properties.

The *CEX2D*[10] and *CEX3D*[11] simulations were developed at the Jet Propulsion Laboratory. These models compute ion particle trajectories in the domain in order to determine the ion current and densities. Both models set an input ion density which determines the output beamlet current. *CEX2D* and *CEX3D* model CEX ion production in a manner similar to *ffx*, and they use a linearized Boltzmann relation to simulate the electron fluid. *CEX3D* is capable of simulating cusp structures on the ion optics, although in this case they are modeled as smooth triangular shapes rather than stair-steps.

One note on the *erode* model is that, for the perveance simulations, neutral particles are not simulated. This allows much faster operation of the code, although it results in no accelerator grid current unless direct impingement is occurring. This is actually somewhat advantageous in this situation, as it allows exact determination of when the onset of direct impingement occurs.

B. Direct Impingement Prediction

For these cases, the ion optics geometry is set to the nominal NEXT geometry, with an 1800 V discharge potential, 1775 V screen grid potential, and -210 V accelerator grid potential. For the *erode* simulation, the downstream plasma potential is set to 15 V, while it is 10 V in the other four models. This is not expected to affect the results significantly, as the electron density is very low in the accelerator grid aperture in either case. No doubly-charged xenon ions are simulated. The *ffx*, *igx*, *CEX2D*, and *CEX3D* simulations were all performed by Farnell and Williams[a].

In Figure 2, the accelerator grid-to-beamlet current ratio is plotted for all five computational models, as a function of beamlet current. Several similarities and differences between the models can be seen. For the low-current cross-over condition, the only two models that predict cross-over at all are the *erode* and *ffx* codes. The other models show no increase in accelerator grid current due to direct ion impingement. Also, there is excellent agreement between the *ffx* and *erode* codes on the point at which cross-over impingement begins, with both predicting this at a current of about 0.02 mA.

[a]Personal Communication, Cody Farnell and John Williams, May 2005

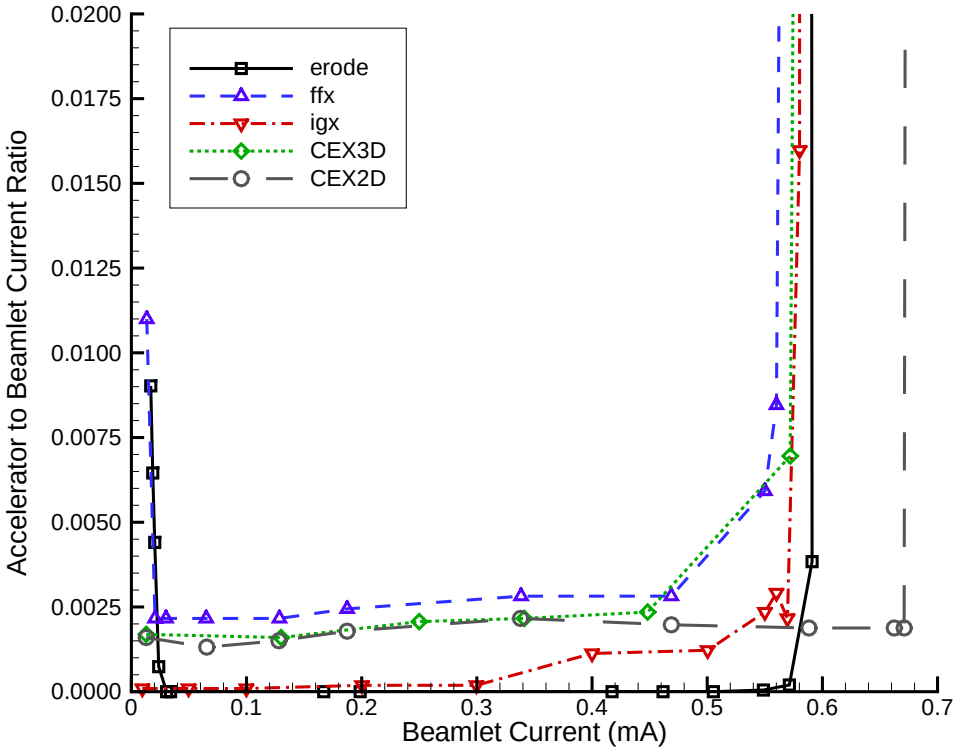

Figure 2. Accelerator grid-to-beamlet current ratio as a function of beamlet current. Results from several computational models are shown.

All simulations predict direct beamlet impingement for currents near the Child's Law limit, although there is some spread in the predictions. The *igx* and *CEX3D* codes show excellent agreement, predicting direct impingement at a current of about 0.57 mA, while the *ffx* model gives direct impingement at a slightly lower beamlet current. The erode model shows direct impingement beginning at about 0.60 mA, while the *CEX2D* code prediction is much higher at 0.67 mA.

The differences between the models may be due to several factors. The electron fluid model may be one of the primary sources of discrepancy, as this strongly affects the shape of the upstream sheath, and thus the focusing of the beamlet. The dimensionality of the simulations would be expected to have a strong effect, but the results do not confirm this. While the 3-D *igx* and *CEX3D* results are very close to each other in terms of the perveance limit, the 2-D *CEX2D* and *erode* models give very different behavior. For the cross-over limit, it is the 2-D *erode* simulation that matches the fully 3-D *ffx* model. The fact that these two codes match at this condition strongly suggests that the use of the full Boltzmann relation is critical in predicting cross-over impingement.

Differences in the simulated geometry can also affect results. The *erode* model uses a uniform, rectangular, mesh to represent the domain and ion optics geometry, giving some small error in the location of boundaries. Cusp geometry is also simulated differently among the models– the *CEX* models have a smooth linear representation of the cusp structures, while the *erode* and *ffx* models represent the cusps as a stair-step pattern.

The current ratio and perveance fraction are plotted as a function of beamlet current in Figure 3 for the *erode* model. The perveance limit is reached at exactly the point predicted by theory– when the beamlet current is such that the perveance fraction is equal to one. Past this point, the perveance fraction increases because the upstream ion density is increased further. However, the output beamlet current decreases due to large amounts of current being collected on the accelerator grid. This is an affirmation that the simulation is accurately modeling the ion optics aperture. The simulation does not allow more than the theoretical maximum amount of current to pass through the optics.

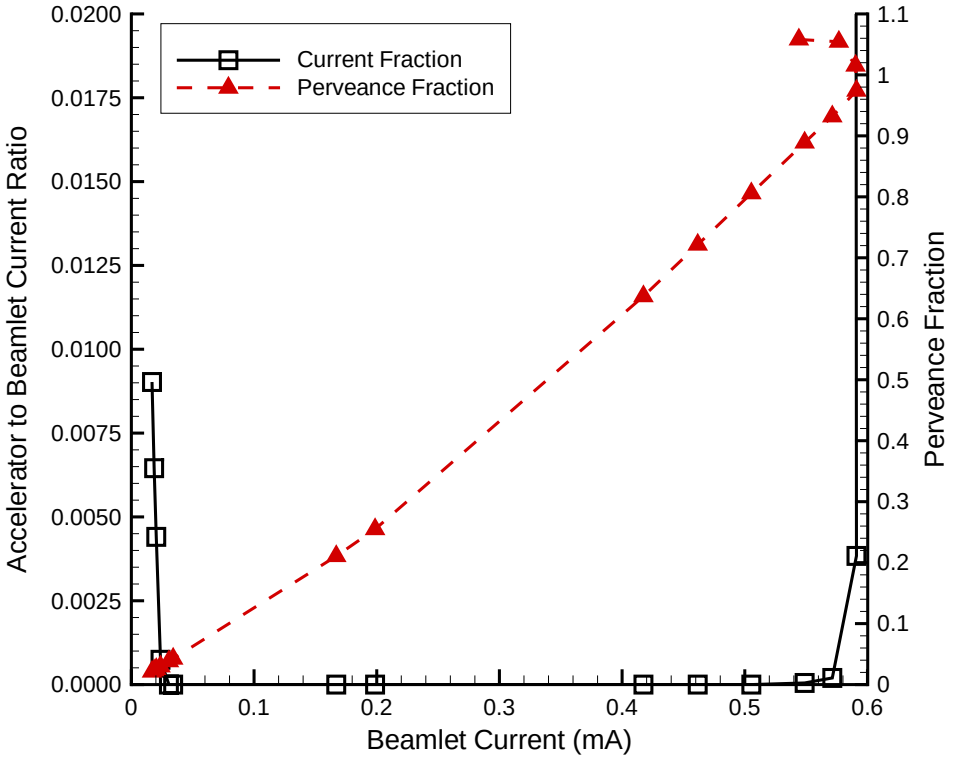

Figure 3. Accelerator grid-to-beamlet current ratio and perveance fraction as a function of beamlet current. The beamlet current decreases after the perveance fraction reaches one because large amounts of current are collected on the accelerator grid.

C. Minimum Centerline Potential

The minimum centerline potential point, also called the saddle point, is the point at which the potential field is lowest on the centerline of an ion optics aperture. The potential drops radially away from this point due to the imposed electric field of the accelerator grid, and the potential increases both upstream and downstream due to the discharge and plume plasma potentials. Thus, the saddle point is the weakest in terms of preventing electron backstreaming. When the minimum centerline potential increases sufficiently due to widening of the accelerator grid aperture, electrons are able to pass through the saddle point and flow into the discharge chamber. From a simulation standpoint, the ability to accurately model the potential at this point is then very important, as it allows prediction of the failure of a thruster due to electron backstreaming.

Figure 4 plots the minimum centerline potential as a function of beamlet current for the different computational models. Again, some differences can be seen between the models, although the general behavior is the same. The 2D *erode* and *CEX2D* models predict almost exactly the same potential at all points, and they are also fairly close to the *CEX3D* results. However, the *ffx* and *igx* models predict saddle point potentials much lower than given by the other models, with the *igx* code giving potentials as much as 30 V lower.

The source of this discrepancy is currently unknown. The potential at this point should be due exclusively to the accelerator grid effect and the ion space charge, thus the electron model should not affect results greatly. Some effect may occur due to differences in ion focusing that results in a lower centerline ion density in the *igx* and *ffx* models. The similarity between the 2-D *CEX2D* and *erode* models is not unexpected, as both have an axisymmetric geometry. It is surprising then that the *igx* potential prediction is so much lower than the *CEX3D* results, as both simulate a similar domain. It is also interesting to note that the 3-D *CEX3D* results are not extremely different from the 2-D results.

For both current ratio and saddle point potential, there is no clear difference between the 2-D and 3-D models. This is encouraging, as it means that a full 3-D model is not necessarily needed for preliminary

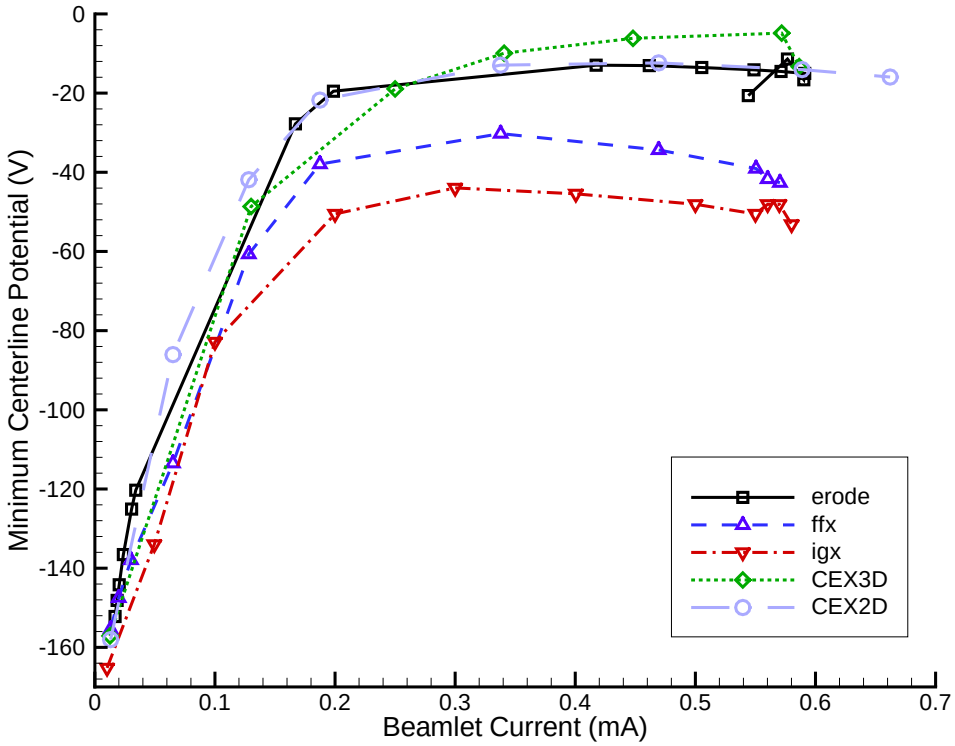

Figure 4. Minimum centerline potential as a function of beamlet current for several computational models. Generally good agreement is seen between the models, although the *igx* and *ffx* models predict lower potentials than the other models for high beamlet currents.

simulations of ion optics behavior. Thus, such simulations can be performed much more rapidly, making a computational model a useful ion thruster design tool.

D. Grid Gap Variation

The spacing between the accelerator grid and screen grid can vary by a large amount between thruster operation and rest. In the center of the optics, the spacing may decrease by 60% from the cold gap value when the beam is extracted. This can have a significant effect on the ion flow in the apertures.

The accelerator-to-beamlet current ratio is plotted in Figure 5 as a function of the grid gap for the *erode* model. Both axes are scaled by the value at the nominal grid gap, and the beamlet current simulated is approximately 0.0237 mA. As the plot shows, small decreases in the gap from the nominal value do not greatly change the current ratio. However, as the gap is decreased further, the increase in the current ratio becomes severe, giving 6 times as much current for a gap half the size of the nominal value.

This illustrates the importance of knowing the grid gap in order to obtain accurate simulations. Even for conditions that are not perveance-limited, the grid gap will have a significant effect on the beamlet divergence. This can affect simulated thrust as well as downstream plasma properties. The importance of grid gap can be seen in Eqn. 1. The perveance fraction depends on the square of the grid gap, so decreasing the gap has a strong effect on the fraction.

E. Discharge Potential Variation

One problem with the perveance results shown above is that they do not correspond to actual thruster operation. Each case simulates a single aperture out of many thousands in the thruster optics. In reality, the perveance behavior of the thruster depends on all apertures, and the variation of beamlet current in each aperture.

Experimentally, the perveance limit is measured by decreasing the discharge potential with a constant beam current until an increase in accelerator grid current is observed. To model this same situation, several

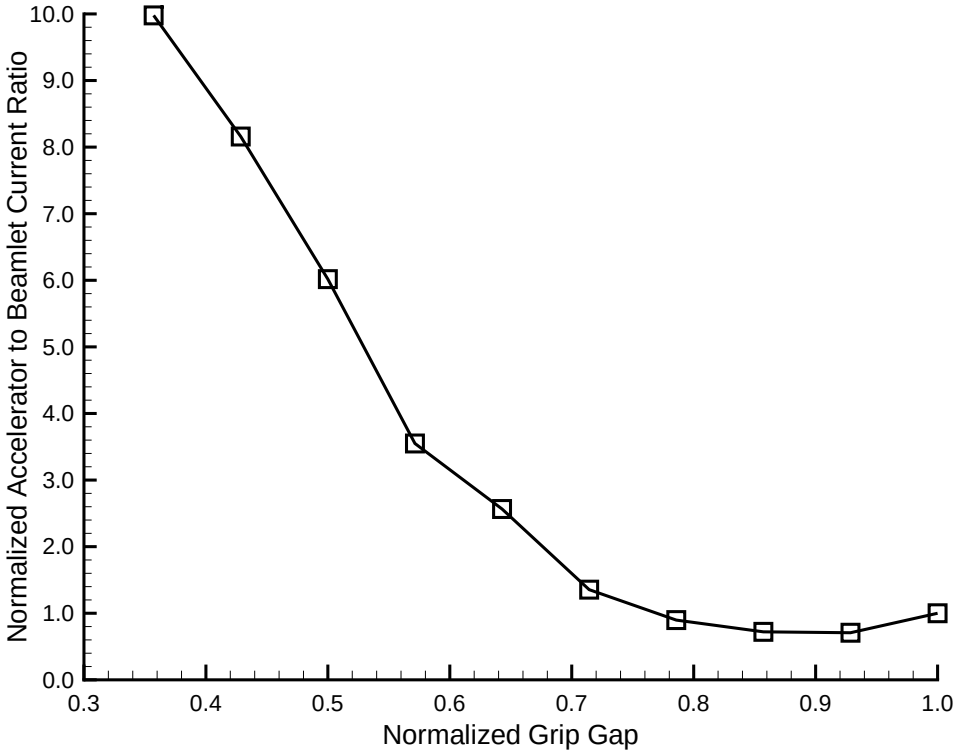

Figure 5. The effect of the grid gap on the accelerator grid-to-beamlet current ratio at a beamlet current of 0.0237 mA. Decreasing the gap by a factor of two increases the current by a factor of six.

simulations are performed with the *erode* code across the thruster face at a given discharge potential, then the results of these simulations are integrated to obtain results for the entire thruster. This method has been used previously in the *erode* model.[12] As in the previous simulations, neutral particles are not simulated in order to allow much shorter simulation running times. For each discharge potential, nine simulations are performed at varying aperture diameters and beamlet currents across the thruster face. The *ffx* model is also used to provide results for a single aperture on the thruster centerline.

Figure 6 plots the simulated accelerator grid-to-beamlet current ratio as a function of total voltage, which is the discharge potential plus the absolute value of the accelerator grid potential. Also shown is the experimental point at which the perveance limit is reached.[1] The *erode* simulation shows some accelerator grid current at the nominal potential due to cross-over impingement in the outer apertures, but this effect does not appear for lower discharge potentials. The *erode* model sees perveance-limited impingement at a total voltage of about 800 V, under-predicting the perveance-limiting potential measured experimentally by 200 V. The experimental limit is reached at a total voltage of about 1050 V. The *ffx* results are somewhat closer to the experimental value, showing impingement starting at about 900 V of total voltage.

The reason for the discrepancy between the simulation results is that the *erode* simulations do not maintain a constant beam current as the discharge potential is decreased. Experimentally, the beam current is held constant, so this increases the required discharge ion density, due to slower moving beam ions as well as a lower screen grid ion transparency. The *ffx* simulations are performed at a constant beamlet current, giving perveance performance closer to the experimental data. The fact that only the centerline aperture is simulated prevents the *ffx* results from more closely matching the experimental data.

IV. Downstream Beamlet Expansion

In a standard axisymmetric ion optics aperture simulation, the upper boundary of the domain is generally considered to be reflective. This means that the simulation domain is effectively a cylinder. Thus, the ion and neutral densities in the domain cannot decrease, no matter how long the domain is. In an actual thruster,

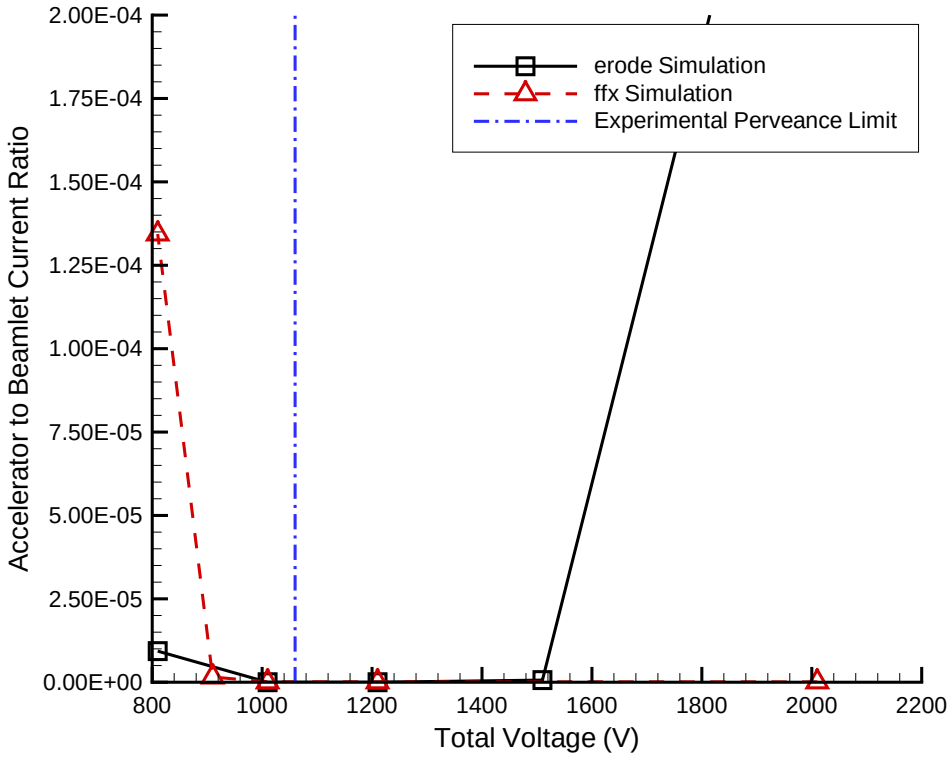

Figure 6. Accelerator grid-to-beamlet current ratio as a function of total voltage for the entire thruster operating at 3.52 A of beam current. The experimental perveance limit is shown as well. The *erode* simulation under-predicts the potential needed to reach the perveance limit by 200 V, while the *ffx* results compare much more favorably.

the beam expands, reducing the density as the distance from the ion optics increases. This drop in ion density leads to a potential hill, preventing charge-exchange ions from reaching the accelerator grid. The reflective boundary condition is justified by the fact that each aperture is surrounded by six other apertures. Each of these apertures is assumed to be producing identical particles as the center aperture, so any particle reaching a boundary would be entering the domain of another cylindrical simulation domain. However, this assumption breaks down for two reasons: first, if each aperture domain is treated as a cylinder, there is space between the cylinders that is not simulated. Ions can expand into this space, reducing the ion density. Second, the area covered by the entire beam of the thruster increases downstream of the optics, again lowering the ion density. There are certainly some particles that would re-enter another cylindrical domain from neighboring apertures, so it would not be correct to assume that all particles should be allowed to pass through the upper boundary. Instead, the amount of particles allowed through should be related to the area increase due to the expansion of the beam.

Such a boundary condition has been imposed for the *erode* model. The thruster divergence is set to a given value prior to the beginning of the simulation. During the simulation, each particle that reaches the upper boundary downstream of the accelerator grid, with a positive axial velocity, is considered for removal from the simulation. The ratio between the non-simulated area and the simulated area of the thruster can be expressed as

$$P_1 = \frac{z_p - z_a}{z_0}\left(\frac{z_p - z_a}{z_0} + 2\right), \tag{4}$$

where

$$z_0 = \frac{r_{beam}}{\tan\left(\theta_{diverge}\right)}, \tag{5}$$

z_p is the axial particle position in the domain, z_a is the axial location of the downstream face of the accelerator grid, r_{beam} is the beam extraction radius of the thruster, and $\theta_{diverge}$ is the divergence angle of the beam.

A second ratio is the velocity angle of the particle, expressed as

$$P_2 = \frac{2}{\pi} \arctan\left(\frac{v}{u}\right). \tag{6}$$

The probability that a particle is removed is set to the product of these two factors, P_1 and P_2. Particles that reach the upper boundary are deleted randomly based on this probability.

Two points should be noted here. First, the area between cylindrically shaped simulation areas is still not accounted for explicitly here. However, this area is covered further downstream as the area of the beam increases, and the beamlets are essentially allowed to expand to fill the non-simulated area. Second, it is not correct to simply delete particles, as they still have a finite contribution to the thrust, beamlet current, and mass flow rate. This can be accounted for by simply keeping track of the properties of deleted particles. This is a feature that can be easily added to the simulation in future work. For the present study, the performance results of the simulations will be ignored. The maximum power operating condition of the NEXT thruster is simulated, and the centerline aperture is modeled in each case, resulting in a nominal beamlet current of 0.168 mA. The downstream plasma potential is set to 16 V, and a 1 eV electron temperature is assumed.

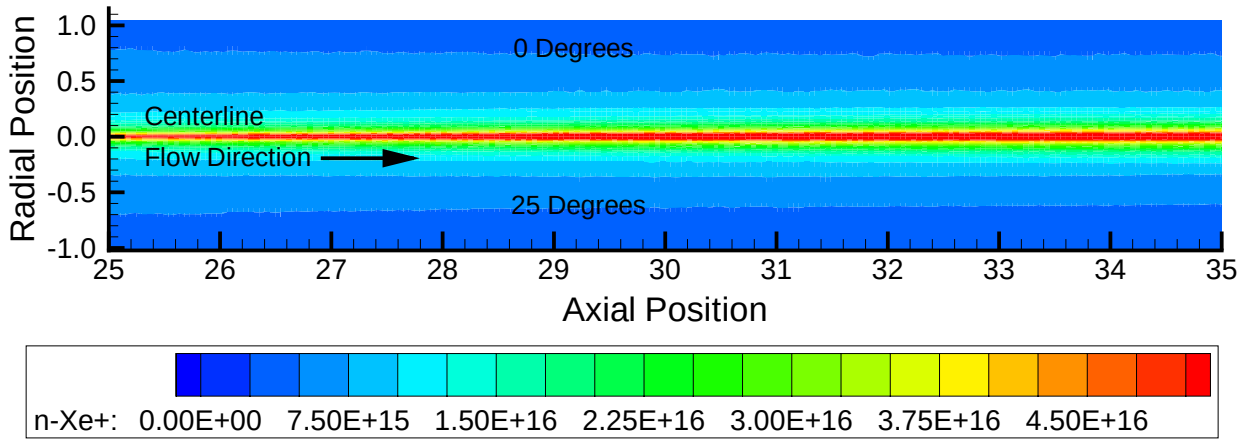

Figure 7. Ion density in the downstream region with and without beamlet expansion. No difference can be seen here because most ions are well-focused by the ion optics, giving very small velocity angles. Thus, few ions reach the upper boundary.

The ion density in the region downstream of the ion optics is plotted in Figure 7. The top half of the plot is the density without beam expansion, while the bottom half is for a beam expansion angle of 25°. The somewhat surprising result is that almost no change can be seen in the ion density. However, if the ion optics operation is considered more closely, this makes sense. The bulk of the ions are focused very tightly for this beamlet current, so very few of them will reach the upper boundary. Those that do will likely have a small velocity ratio, decreasing the odds of deletion. For a case with a higher or lower beamlet current, the ions would not be as tightly focused, leading to a much larger difference in ion density. There is some variation in ion density, however the large gradient in density from the centerline to the outer edge of the domain tends to mask the differences.

Figure 8 plots the axial velocity in the downstream region for the same cases as above. A dramatic difference is seen between the case with expansion and the case without. When no expansion is allowed, particles with a high velocity ratio stay in the domain. This leads to a decrease in average axial velocity on the beamlet centerline. However, when these particles are removed via beam expansion, the velocity is able to maintain high values, and even increases further downstream, as more particles with high velocity angles are removed. Unlike the case of the density, the velocity gradients in the region are much smaller, allowing easier visualization of the difference in velocity.

The neutral density in the downstream region is shown in Figure 9. A significant difference between the expanded case and the confined case is seen, as the neutral density drops by 30% or more for the case with expansion. This is expected, as the neutral population has a much more random velocity distribution, so the neutral plume should expand much more rapidly than the ion plume. This will of course lower the charge-exchange ion creation rate in the simulation, in turn lowering the accelerator grid current simulated.

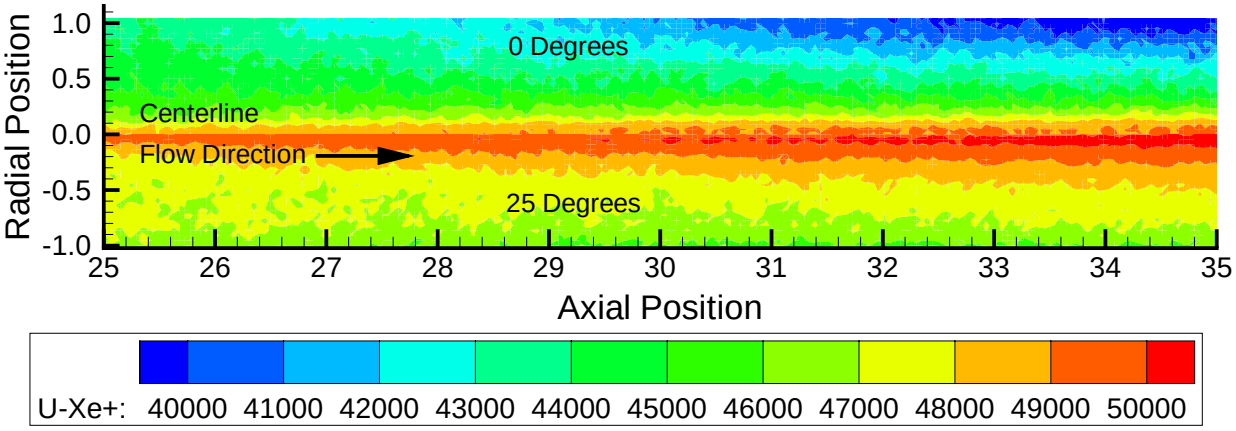

Figure 8. Axial velocity in m/s in the downstream region with and without beamlet expansion. The average velocity increases with beamlet expansion because the ions with lower axial velocities typically have higher radial velocities, leading to deletion at the boundary.

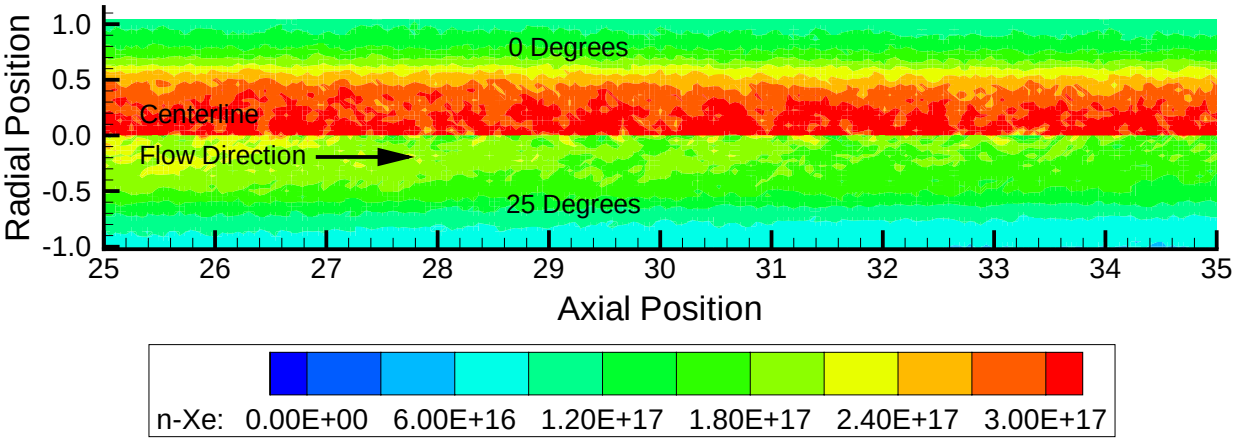

Figure 9. Neutral density in the downstream region with and without beamlet expansion. The neutral density drops by a large amount when the beamlet is expanded. This is due to the highly thermal nature of the neutral particles, as many will have high velocity angles, causing them to reach the upper boundary and be removed from the simulation.

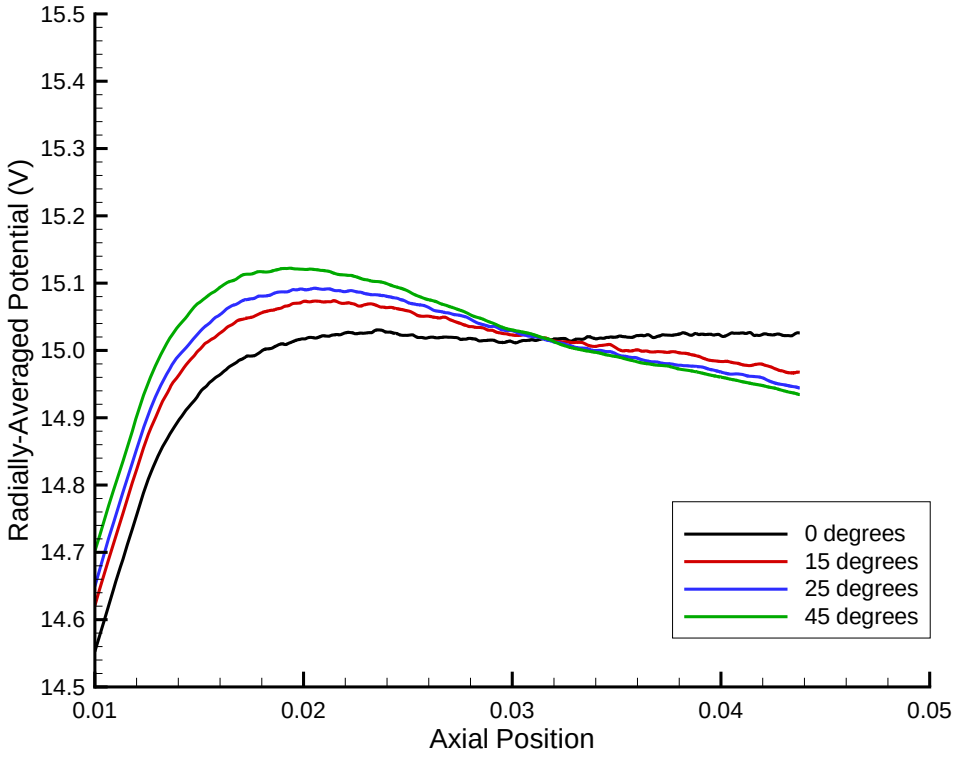

Figure 10. Radially averaged potential field as a function of axial position. The potential is shown for several thruster divergence angles. For any divergence at all, a potential hill forms which will prevent or retard CEX ions from reaching the accelerator grid.

This effect is realistic to an extent, because the neutrals are expanding faster than the ions in the actual thruster, so that there will be regions with neutrals, but no ions. This is offset in regions where ions have expanded as well, due to increased area for CEX collisions to occur.

Figure 10 plots the radially-averaged potential field in the computational domain as a function of axial position. Each point is the result of area-weighted averaging of the potential field in the domain for each axial position. At the beginning of the plot, the potential field is increasing after leaving the area of effect of the accelerator grid. As the axial position increases, the potential rises to the potential of the neutralizing electrons. For the case without beamlet expansion, the averaged potential reaches 15 V and levels off, showing no increase or decrease after that point. When expansion is enabled, the potential increases beyond the downstream plasma potential, then decreases again as the axial location increases. For higher beam expansion angles, the effect becomes more pronounced.

This effect is what occurs in reality in the thruster, where any CEX ions created downstream of the potential hill are unable to reach the accelerator grid. Although the changes in potential are small at less than 0.3 V on the plot, this is sufficient to stop, or at least slow, a CEX ion with a thermal velocity from reaching the accelerator grid.

The reason for the formation of this hill in the simulation is based on the Boltzmann equation, which is used to model the electron fluid:

$$n_e = n_{e,0} \exp\left(\frac{\phi - \phi_0}{T_{e,0}}\right). \tag{7}$$

Here, $n_{e,0}$ is the reference electron density, ϕ_0 is the downstream plasma potential, and $T_{e,0}$ is the reference electron temperature. In the simulation, the plasma at the downstream boundary is assumed to be neutral, so the reference electron density is set to the average ion density near the downstream edge of the domain. In a simulation without expansion, the average ion density does not vary outside of the accelerator grid aperture, thus a neutralized plasma potential is reached not far downstream of the aperture. In the cases with expansion, the ion density is higher near the aperture exit than it is at the downstream boundary. This results in a lower reference density for the neutralizing electrons, so the potential is able to increase near

the aperture exit. Further downstream the ion density drops due to expansion, while the reference electron density remains constant, such that the potential decreases.

In an ironic twist, this kind of boundary condition and beamlet behavior is easier to simulate in an axisymmetric domain than in most 3-D domains. With the exception of the *ffx* model, most 3-D simulations make use of symmetry to reduce the domain that needs to be simulated, however this has the result that no boundary is an "outer" boundary, where ions could be deleted to model beamlet expansion.

V. Conclusions

Two primary ion optics phenomena were explored in this paper. The prediction capabilities of several models were compared and contrasted for the perveance behavior of the optics as the beamlet current was varied. Although there were differences between the models in both accelerator-to-beamlet current ratio and minimum centerline potential, the models in general showed fairly good agreement with each other. The importance of the grid gap in determining the cross-over limit was illustrated as well, with the cross-over current increasing by a factor of six for a reduction in gap of a factor of 0.5. The perveance limit was also examined for the entire thruster with varying discharge potential in order to directly compare to experimental results. This showed a large difference between the experiment and the *erode* simulation prediction, although this is most likely due to a low simulation current density.

The effect of a beamlet expansion boundary condition was also examined. Such a boundary condition does not strongly affect the ion density in the domain, but the average axial ion velocity is increased in the simulation domain, and the neutral density is strongly reduced. The potential field is altered when beamlet expansion is employed such that it behaves in a more realistic way. A potential hill is formed downstream of the accelerator grid, preventing or retarding CEX ions from reaching the accelerator grid.

Acknowledgements

Support for this work is provided in part by NASA Glenn Research Center Grant NAG3-2497 with Jon Van Noord as the technical monitor. Support is also provided by a Michigan Space Grant Consortium Graduate Student Fellowship.

References

[1]Soulas, G. C., Kamhawi, H., Patterson, M. J., Briton, M. A., and Frandina, M. M., "NEXT Ion Engine 2000 Hour Wear Test Results," AIAA 2004-3791, 40th AIAA/ASME/SAE/ASEE Joint Propulsion Conference, Fort Lauderdale, FL, July 2004.

[2]Frandina, M. M., Arrington, L. A., Soulas, G. C., Hickman, T. A., and Patterson, M. J., "Status of the NEXT Ion Thruster Long Duration Test," AIAA 2005-4065, 41st AIAA/ASME/SAE/ASEE Joint Propulsion Conference, Tucson, AZ, July 2005.

[3]Emhoff, J. W. and Boyd, I. D., "Grid Erosion Modeling of the NEXT Ion Thruster Optics," AIAA 2003-4869, 39th AIAA/ASME/SAE/ASEE Joint Propulsion Conference, Huntsville, AL, July 2003.

[4]Emhoff, J. W. and Boyd, I. D., "Progress in NEXT Ion Optics Modeling," AIAA 2004-3786, 40th AIAA/ASME/SAE/ASEE Joint Propulsion Conference, Fort Lauderdale, FL, July 2004.

[5]Farnell, C. C., Williams, J. D., and Wilbur, P. J., "NEXT Ion Optics Simulation Via ffx," AIAA 2003-4869, 39th AIAA/ASME/SAE/ASEE Joint Propulsion Conference, Huntsville, AL, July 2003.

[6]Birdsall, C. K. and Langdon, A. B., *Plasma Physics Via Computer Simulation*, Adam Hilger Press, 1991.

[7]Bird, G. A., *Molecular Gas Dynamics and the Direct Simulation of Gas Flows*, Oxford University Press, 1994.

[8]Monheiser, J. M., "Development and Verification of a Model to Predict Impingement Currents for Ion Thrusters," CR 195322, NASA, 1994.

[9]Nakayama, Y. and Wilbur, P. J., "Numerical Simulation of Ion Beam Optics for Many-grid Systems," *AIAA Journal of Propulsion and Power*, Vol. 19, No. 4, 2001, pp. 607–613.

[10]Brophy, J. R., Katz, I., Polk, J. E., and Anderson, J. R., "Numerical Simulations of Ion Thruster Accelerator Grid Erosion," AIAA 2002-4261, 38th AIAA/ASME/SAE/ASEE Joint Propulsion Conference, Indianapolis, IN, July 2002.

[11]Anderson, J. R., Katz, I., and Goebel, D., "Numerical Simulation of Two-Grid Ion Optics Using a 3D Code," AIAA 2004-3782, 40th AIAA/ASME/SAE/ASEE Joint Propulsion Conference, Fort Lauderdale, FL, July 2004.

[12]Emhoff, J. W. and Boyd, I. D., "NEXT Ion Optics Modeling of Total Thruster Performance," AIAA 2005-3687, 41st AIAA/ASME/SAE/ASEE Joint Propulsion Conference, Tucson, AZ, July 2005.